

# **NANOIDENTIFICATION OF POLYMERS: OVERVIEW**

by

**Mark R. VanLandingham and John S. Villarrubia**  
**Building and Fire Research Laboratory**  
**National Institute of Standards and Technology**  
**Gaithersburg, MD 20899, USA**

and

**Gregory F. Meyers**  
**Dow Chemical Company**  
**1897E Building**  
**Midland, MI 48677, USA**

Reprinted from the ACS Polymer Preprints, Vol. 41, No. 2, 1412-1413, 2000.

**NOTE:** This paper is a contribution of the National Institute of Standards and Technology and is not subject to copyright.



**NIST**

**National Institute of Standards and Technology**  
Technology Administration, U.S. Department of Commerce

## NANOINDENTATION OF POLYMERS: OVERVIEW

Mark R. VanLandingham\*, John S. Villarrubia\*, and Gregory F. Meyers\*\*

\* National Institute of Standards and Technology, 100 Bureau Drive,  
Gaithersburg MD 20899

\*\* Dow Chemical Company, 1897E Building, Midland, MI 48677

### Introduction

Depth-sensing indentation devices allow the amount of penetration of an indenter into a material to be measured as a function of applied load<sup>1,2</sup>. The objective of micro- and nanoindentation testing using these devices is to produce absolute measurements of material properties under indentation loading. Further, the ability of these devices to measure the responses of microscopic regions can be a key to understanding mechanical behavior of technologically important material systems. However, many polymers are too soft for their indentation responses to be measured using these devices because the system compliance is too low<sup>3</sup>. Even for polymers with modulus values greater than 1 GPa, producing indents with both lateral and depth dimensions much less than 1  $\mu\text{m}$  is difficult, particularly because these devices, in general, cannot detect initial contact loads less than 1  $\mu\text{N}$ . Thus, these systems have limited capabilities for studying polymer thin films, polymer composites, and other important polymer systems.

The atomic force microscope (AFM) is useful for evaluating polymeric materials on a sub-micrometer scale. AFM images are produced by scanning a probe, consisting of a sharp tip (nominal tip radius on the order of 10 nm) located near the end of a cantilever beam, across a sample surface using piezoelectric scanners. The AFM can also be operated in a non-imaging mode, called force mode, to perform indentation tests. A force curve is produced, which is a plot of tip deflection as a function of the vertical motion of the scanner. This curve can be analyzed to provide information on the local mechanical response<sup>4,6</sup>. Also, the spring constant of the cantilever probe can be chosen such that small differences in response can be detected between polymers that have a certain range of stiffness<sup>4</sup>.

AFM indentation measurements are relative measurements, largely due to the lack of information regarding the tip shape of the AFM probes. Also, current tip shape calibration procedures used in depth-sensing indentation rely on indentation results from a reference material, and the reproducibility of these methods has been poor in a recent interlaboratory comparison<sup>7</sup>. In this paper, a technique referred to as blind reconstruction is used as a material-independent method for characterizing the tip shapes of probes used with the AFM to indent polymeric materials. Results using this method are compared to results of a material-dependent tip shape analysis.

### Experimental

**Materials.** A benzocyclobutene (BCB) polymer (Cyclotene 5021, Dow Chemical<sup>8</sup>) was prepared by the manufacturer as a smooth film by spin casting from a partially cured (B-stage) solution in mesitylene onto a thermal oxide silicon wafer. The B-staged material had been taken to a state of 40 % cure with a mass fraction of solids of 0.63. Spin casting at 323 rad/s (3085 rpm) for 30 s was followed by curing at 250 °C for 60 min, all in a nitrogen atmosphere. Film thickness was measured using ellipsometry to be 11.0  $\mu\text{m}$   $\pm$  0.4  $\mu\text{m}$ . From AFM results utilizing phase contrast imaging, heterogeneity in this sample was not observed, and root-mean-square roughness, measured using 5  $\mu\text{m}$  x 5  $\mu\text{m}$  AFM images, was found to be 6 nm  $\pm$  0.5 nm. The room-temperature tensile modulus was reported by the manufacturer to be approximately 2.9 GPa and the glass transition temperature, measured using differential scanning calorimetry, was in excess of 350 °C.

**Instrumentation.** Indentation of the BCB polymer sample was performed using two different AFM indentation systems. The first system was a Dimension 3100 AFM (Digital Instruments<sup>8</sup>). A diamond-tipped stainless steel cantilever was used as the indentation probe using a technique described in detail elsewhere<sup>4,6</sup>. The spring constant of this probe was measured by the manufacturer (Digital Instruments<sup>8</sup>) to be 120 N/m  $\pm$  10 N/m. Three sets of indentation measurements were made with each set containing one indent at eight load levels ranging from 1.4  $\mu\text{N}$  to 13.7  $\mu\text{N}$ . The measured load-penetration responses at each force level were used to produce an estimation of the tip shape using indentation tip shape calibration procedures (see Reference 1).

The second system was a Triboscope (Hysitron<sup>8</sup>) depth-sensing indentation system mounted on a Multimode AFM (Digital Instruments<sup>8</sup>). When interfaced with an AFM, the transducer/indenter tip assembly replaces the AFM cantilever probe assembly. A Berkovich-type indentation tip was used for imaging and indentation. Imaging was performed with this tip in contact with the sample under a constant applied load of approximately 1  $\mu\text{N}$ , as measured by the transducer and used as feedback to the AFM scanner. Tip shape calibration (see Reference 1) was performed by analyzing a set of 28 load-penetration curves on fused silica with maximum loads of between 25  $\mu\text{N}$  and 5200  $\mu\text{N}$ . For most of the load levels, two or more load-penetration curves were analyzed. Indentation of the BCB sample was then performed using maximum loads similar to those used for tip shape calibration.

Prior to the tip shape calibration measurements, load-frame compliance was calibrated for both indentation systems. This calibration allows the displacement of the load frame to be removed from the total measured displacement so that only displacement due to penetration of the tip into the sample remains. For the AFM cantilever probe, a sample that is stiff with respect to the probe is used, as is described in detail elsewhere<sup>4,6</sup>. For each of the eight load levels used to indent the BCB sample, 10 force curves were obtained on a smooth sapphire sample, five directly before and five directly after indenting the BCB sample, using the same probe and operating conditions. For the depth-sensing indenter, load frame compliance was calibrated by indenting fused silica at load levels ranging from 3000  $\mu\text{N}$  to 5200  $\mu\text{N}$  using the manufacturer's recommended procedure. A total of 11 indentation curves were analyzed.

**Blind Reconstruction.** At each pixel in any topographic AFM image, information is contained about the tip geometry as well as the sample surface<sup>9</sup>. To extract the part concerning the tip, topographic AFM imaging can be modeled in terms of the set of points,  $I$ , on or below the image surface, a similar set of points,  $S$ , describing the sample, the set of points,  $P$ , describing the reflection of the tip through the origin, and the mathematical morphology dilation operator,  $\oplus$  as  $I = S \oplus P$ <sup>10-12</sup>. To the extent that this model is realistic, the tip geometry can be determined from an unknown experimental sample's image<sup>10,11</sup>. However, the tip shape determined after consideration of all image points is an outer bound on the true tip shape, and the sharpest features on the specimen determine the accuracy of the 3-dimensional tip shape information. Also, this dilation model is an approximation, as the real image includes non-tip artifacts such as noise, scanner nonlinearity, and feedback loop response time. These instrumental artifacts produce sharp spikes in the image that cannot be entirely removed by filtering. To limit the influence on the tip estimate of these small deviations from the model, a threshold parameter is used that describes the maximum amount by which the image deviates from an ideal dilation<sup>12</sup>.

**AFM Imaging of Tip Shape Characterizers.** AFM images of three samples, which are often referred to as tip shape characterizers, were used to estimate the shapes of indenter tips using blind reconstruction. Imaging was performed with a diamond-tipped stainless steel cantilever probe in tapping mode, and also with the Berkovich indenter tip in contact mode. Images with scan sizes of 1  $\mu\text{m}$  x 1  $\mu\text{m}$  and 5  $\mu\text{m}$  x 5  $\mu\text{m}$  consisting of 512 scan lines, each line with 512 pixels, and taken at a scan rate of 1 Hz, were made for each tip-sample combination. Two of the samples, described as roughness-type characterizers, were rough columnar thin films of niobium and titanium, respectively (General Microdevices<sup>8</sup>). The other sample was a silicon grating (ND-MDT<sup>8</sup>) that contained an array of spike-like features with symmetric tip sides, a tip angle of less than 20°, and a tip radius of curvature of less than 10 nm (manufacturer's specifications). While the features of the roughness samples can be sharp relative to the spikes, the largest features are not particularly large, and thus images of these samples were used only to reconstruct a portion of the tip near the apex. Because the spike features are much taller, the spike characterizer was used to reconstruct the portion of the tip away from the apex that was not accessible to the roughness samples.

### Results and Discussion

An image created by scanning the spike characterizer sample with the Berkovich tip is shown in Figure 1. The spikes essentially image the tip such that the Berkovich tip geometry, broadened by the finite size of each spike, is produced several times in the image. The area-depth relationship for this tip was calculated from blind reconstruction results. In Figure 2, this result is compared to that from an indentation tip-shape analysis, in which fused silica was indented using a range of applied loads with this same Berkovich tip.

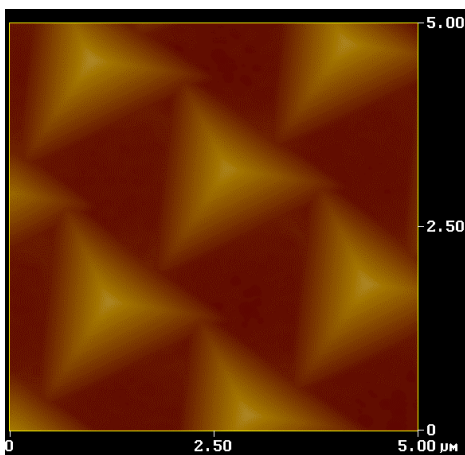


**Figure 1.** AFM topographic image generated by scanning the spike characterizer sample with a Berkovich indentation tip (color contrast from black to white represents a total range of 1.2  $\mu\text{m}$ ).

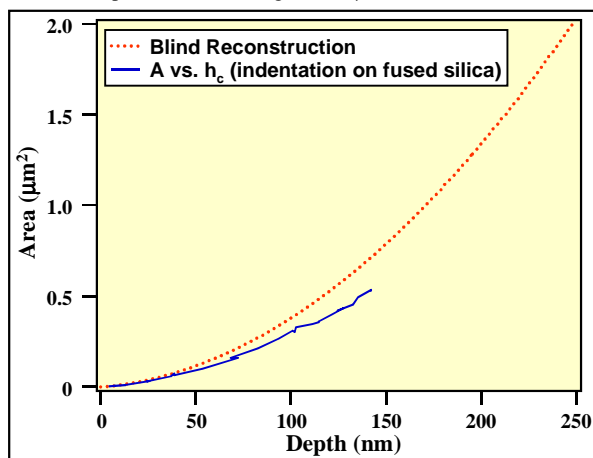


**Figure 2.** Area vs. depth for the Berkovich tip; comparison of blind reconstruction results to results from an indentation tip-shape analysis.

In a similar study, the diamond-tipped AFM cantilever was used to scan the tip characterizer samples and indent the BCB polymer using a range of applied loads. In Figure 3, the area-depth relationships calculated from the blind reconstruction results and from a tip-shape analysis using the polymer indentation results are compared. In both Figures 2 and 3, significant discrepancies are observed between the two methods of tip shape characterization. However, these results are preliminary, and a thorough analysis of measurement uncertainties for the two methods has yet to be completed. Uncertainties in the blind reconstruction results include (1) the sizes of the sharpest features of the characterizer samples, particularly with regard to the spike characterizer, which may be more susceptible to damage during imaging; (2) non-tip image artifacts and the choice of the threshold parameter used to reduce the influence of those artifacts; and (3) for the depth-sensing indenter, slight deviations from perpendicularity of the tip with respect to the characterizer sample.

In general, uncertainties in the blind reconstruction area measurements in Figures 2 and 3 are estimated to be less than  $\pm 5\%$  of each calculated value, although current efforts involve a more complete uncertainty analysis. However, the uncertainties in the indentation tip shape analyses could be much larger<sup>5,7</sup>. For the depth-sensing indenter, these uncertainties include (1) load-frame compliance calibration; (2) detection of a true zero in load and displacement; (3) uncertainties associated with curve fitting; (4) uncertainties in the elastic modulus of fused silica; and (5) uncertainties related to differences between elasticity theory and real material behavior. For the AFM, uncertainties include (1) lateral forces acting on the tip due to cantilever

bending; (2) scanner and photodiode nonlinearities; (3) uncertainties associated with curve fitting; and (4) time-dependent deformation behavior of the polymer.

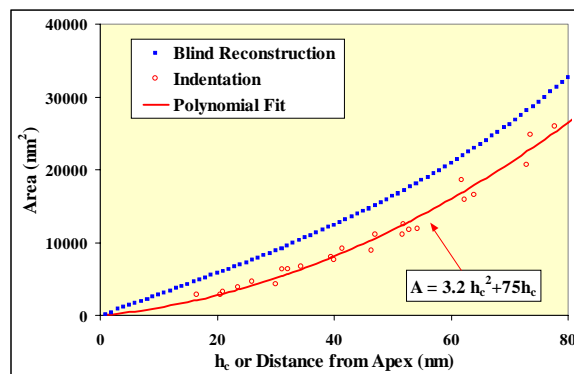


**Figure 3.** Area vs. depth for the AFM diamond tip; comparison of blind reconstruction results to results from an indentation tip-shape analysis.

Direct comparisons between the two methods of tip shape calibration are not possible until complete uncertainty analyses of the indentation measurements are available. Interestingly, however, measurements of elastic modulus,  $E$ , for the BCB polymer were made using both the depth-sensing indenter and the AFM. For the AFM,  $E = 2.1 \text{ GPa} \pm 0.2 \text{ GPa}$  using the blind reconstruction results. For the depth-sensing indenter,  $E = 3.7 \text{ GPa} \pm 0.2 \text{ GPa}$  using the indentation tip shape calibration. In both cases, the uncertainty expressed is the estimated standard deviation from numerous indentation measurements. The tensile modulus measured by the manufacturer was  $E = 2.9 \text{ GPa}$ . Thus, both sets of indentation measurements are in reasonable agreement with the bulk tensile measurement.

### Summary and Conclusions

In this study, blind reconstruction was used to estimate the shape of an AFM diamond probe tip and a tip with Berkovich geometry used with AFM-based indentation systems. In both cases, large deviations were observed between area functions measured using blind reconstruction and those measured using indentation tip-shape calibration. These differences might be due to large uncertainties in the indentation measurements. However, direct comparisons between the two methods of tip shape calibration are not currently possible due to incomplete uncertainty analyses.

### References

- (1) Oliver, W. C.; Pharr, G. M. *J. Mater. Res.* **1992**, *7*, 1564.
- (2) Corcoran, S. G.; Colton, R. J.; Lilleodden, E. T.; Gerberich, W. W.; *Phys. Rev. B* **1997**, *55*, 57.
- (3) Lucas, B. N.; in *Thin-Films -- Stresses and Mechanical Properties VII* **1998**, *505*, 97.
- (4) VanLandingham, M. R.; McKnight, S. H.; Palmese, G. R.; Elings, J. R.; Huang, X.; Bogetti, T. A.; Eduljee, R. F.; Gillespie Jr., J. W.; *J. Adhesion* **1997**, *64*, 31.
- (5) VanLandingham, M. R.; *Microscopy Today* **1997**, *10*, 12.
- (6) VanLandingham, M. R.; Dagastine, R. R.; Eduljee, R. F.; McCullough, R. L.; Gillespie, Jr., J. W.; *Composites Part A* **1999**, *30*, 75.
- (7) Jennett, N. M.; Meneve, J.; in *Fundamentals of Nanoindentation and Nanotribology* **1998**, *522*, 239.
- (8) Certain commercial instruments/materials are identified in this paper to adequately describe the experimental procedure. In no case does such identification imply recommendation or endorsement by the National Institute of Standards and Technology, nor does it imply that the instruments/materials are necessarily the best available for the purpose.
- (9) Montelius, L.; Tegenfeldt, J. O.; *Appl. Phys. Lett.* **1993**, *62*, 2628.
- (10) Villarrubia, J. S.; *Surf. Sci.* **1994**, *321*, 287.
- (11) Bonnet, N.; Dongmo, S.; Vautrot, P.; Troyon, M.; *Microsc. Microanal. Microstruct.* **1994**, *5*, 477.
- (12) Villarrubia, J. S.; *J. Res. Natl. Inst. Stand. Technol.* **1997**, *102*, 425.